

# Treatment of Contaminated Bone Defects With Clindamycin-Reconstituted Bone Xenograft-Composites

Long Bi, Yunyu Hu, Hongbin Fan, Guolin Meng, Jian Liu, Dan Li, Rong Lv

Institute of Orthopaedics and Traumatology, Xijing Hospital, The Fourth Military Medical University, Xi'an, People's Republic of China

Received 15 May 2006; revised 8 October 2006; accepted 16 October 2006  
Published online 1 March 2007 in Wiley InterScience (www.interscience.wiley.com). DOI: 10.1002/jbm.b.30747

**Abstract:** Contaminated or infected bone defects and osteomyelitis after trauma are frequently encountered in clinical practice. It is difficult to make a successful bone graft and control infection at the same time. To find a better method to resolve this dilemma, we prepared a novel clindamycin-reconstituted bone xenograft-composite (C-RBX-C) that comprised of crude bBMP (bovine bone morphogenetic protein), clindamycin, and cancellous bone scaffold, and investigated the morphology, biocompatibility, antibiotic release profile and osteoinductive potential of this composite. The ultrastructure of C-RBX-C was evaluated by scanning electron microscopy; the biocompatibility and osteoinductive potential were assessed by testing ectopic implants. The antibiotic release profile was evaluated using a disc-diffusion assay. Finally, this composite was used to repair a *Staphylococcus aureus* contaminated bone defect in a rabbit model. 16 weeks after the implantation of C-RBX-C, the radial defect had been completely recuperated, with significantly better formation of lamellar bone and recanalization of the marrow cavity, than in the controls (scaffolds without clindamycin or bBMP). These results demonstrate that our novel composite, with its concomitant osteoinductive and antibiotic properties, has significant potential for the treatment of contaminated or infected bone defects and osteomyelitis. © 2007 Wiley Periodicals, Inc. *J Biomed Mater Res Part B: Appl Biomater* 82B: 418–427, 2007

**Keywords:** bioactive material; drug delivery/release; bone graft

## INTRODUCTION

Open fracture frequently results in contaminated or infected bone defects and osteomyelitis after trauma. It is difficult to make effective bone transplantation and treat infection at the same time. Because infection is favored by devitalization of bone, soft tissue, and loss of skeletal stability, systemic administration of antibiotics cannot get approved for local drug concentration and long-term administration may give rise to side-effects such as myelosuppression, nephrotoxicity, and drug-induced hepatitis. Other conventional treatments, such as surgical debridement and suction-irrigation, can only control local infection. For the patients with bone defect, these treatments must have two stages, that is, control of infection at first and bone graft later.<sup>1–3</sup> Therefore, the costly expenses and being kept in bed for extended period make patients suffer.

In recent years, diverse controlled local drug (antibiotic) delivery systems (LDDS) have been developed as treatment

modalities in infectious bone injury or chronic osteomyelitis.<sup>4–7</sup> For the past 20 years, antibiotic-impregnated polymethylmethacrylate (PMMA) bead chains have been used in the treatment of contaminated or infected bone defect and implant-associated osteomyelitis, with good results.<sup>8,9</sup> However, PMMA bead chains exhibit distinct disadvantages, such as potential thermal necrosis and monomer toxicity.<sup>10</sup> Moreover, these bead chains are nonbiodegradable requiring removal at a subsequent operation.<sup>11</sup> With the development of material technology, biodegradable materials, such as bioceramics,<sup>12,13</sup> polymers,<sup>14,15</sup> and composites<sup>16</sup> have been used as LDDS. While different from others, the LDDS for treating the bone defect after surgical debridement of contaminated or infective fractures and osteomyelitis, requires special properties, such as effective bone grafting or repair capabilities, ossification, or osteoinductive and osteoconductive ability.

Autologous cancellous bone graft remains the most effective grafting material for bone defects because it provides the three elements required for bone regeneration: osteoconduction, osteoinduction, and osteogenic cells.<sup>17,18</sup> To overcome the limitations of autografts, such as limited supply and secondary damage, it might be preferable to prepare materials mimicking natural bone in terms of both composition and architecture.

Correspondence to: Y. Hu; e-mail: orth1@fmmu.edu.cn  
Contract grant sponsor: National High Technology Research and Development Program of China; contract grant number: 01Z079

© 2007 Wiley Periodicals, Inc.

We have developed a biological composite, termed reconstituted bone xenograft (RBX),<sup>19</sup> by chemically treating fresh calf cancellous bone to make it an antigen-free carrier and combining it with an extract of calf cortical bone, derived bovine bone morphogenetic protein (bBMP), as a strong osteoinductive growth factor.<sup>20–22</sup> Reconstitution of the two components resulted in a composite with strong osteoinductive activity without evoking an immune rejection. This composite has a natural microstructure, is biodegradable and biocompatible, and exhibits excellent mechanical property.<sup>23</sup>

Based on the studies of RBX, we developed a novel antibiotic containing clindamycin-RBX-composite (C-RBX-C). In evaluating this new composite, we hypothesized that C-RBX-C, with its controlled antibiotic release kinetics, osteoinductive capabilities, good porosity and osteogenesis-matched degradation properties, could concomitantly control infection and repair bone defects at the same time when implanted in contaminated bone segmental defects.

To test this hypothesis, we manufactured C-RBX-C, and then tested and examined its antibiotic release profile and ectopic bone formation capabilities. Subsequently, C-RBX-C was implanted into segmental radial defects in a rabbit model. We specifically evaluated the ability of C-RBX-C to treat contaminated or infected bone defects and osteomyelitis.

## MATERIALS AND METHODS

### Preparation of Crude Bone Morphogenetic Protein Extracts

Crude extracts of bovine bone morphogenetic protein (bBMP) were extracted from fresh calf cortical bone according to Urist et al.<sup>24,25</sup> with slight modifications. Briefly, 6 kg bovine cortical bone were crushed into pieces ( $\sim 6 \text{ mm}^3$ ), demineralized in hydrochloric acid at  $2^\circ\text{C}$  for 72 h, and sequentially extracted in 8M lithium chloride for 6 h and 300 mM  $\text{CaCl}_2$  for 24 h. The matrix was then incubated in water at  $55^\circ\text{C}$  for 6 h and extracted in 6M urea for 24 h. Then, the pellets of cortical bone were filtrated and removed. Then, extracts were dialyzed against urea in distilled water at  $2^\circ\text{C}$  for 24 h and centrifuged at 40,000g for 30 min. The deposition was dissolved in 4M guanidine hydrochloride and centrifuged at 20,000g for 15 min. Finally, the supernatant was filtered through a cellulose acetate membrane (pore size,  $0.30 \mu\text{m}$ ); the filtrate was dialyzed against guanidine hydrochloride in 0.25M citric acid. Electrophoresis in SDS-PAGE showed that it had the same pattern as that already reported.<sup>20–22,26</sup> The extract was finally lyophilized, weighed (2.85 g purified “crude BMP” extract was obtained), and stored in sealed sterile containers. To evaluate its biologic activity, 2 mg of the final product was enveloped by gelatin sponge for slow-release of bBMP and was implanted into the right thigh muscle pouches of mice ( $n = 12$ ) for the bioassay described below.

### Treatment of Calf Cancellous Bone

Calf cancellous bone was minced into  $5 \text{ cm}^3$  granules and rinsed in distilled water at  $50^\circ\text{C}$ . After removal of the fat with a 1:1 (v/v) mixture of chloroform/methanol for 12 h, the granules were deproteinized with 8.8M hydrogen peroxide for 48 h followed by immersion in 0.6M hydrochloric acid at  $2^\circ\text{C}$  for 3 min for partial decalcification.

### Preparation of Reconstituted Bone Xenografts

Four hundred mg of the crude bBMP extract was dissolved in 2M guanidine hydrochloride. Two gram of partially decalcified cancellous bone granules were added under mild vacuum of  $-0.08 \text{ MPa}$ . Each granule contained 1.5 mg of crude bBMP. For each experiment 30 mg of the resulting material, designated henceforth as “reconstituted bone xenograft” (RBX), was dialyzed against distilled water for 72 h, lyophilized (This is a common method for loading porous scaffolds with bone-inducing proteins.<sup>27,28</sup>) and sterilized with ethylene oxide.

### Preparation of Clindamycin-Reconstituted Bone Xenograft-Composites

Gelatin, dehydrated glycerol, and distilled water were mixed at a ratio of 3:1:6 (v/v/v) and kept in an  $80^\circ\text{C}$  water bath to make a gelatin solution. Clindamycin powder (Sine Pharmaceutical Factory, Shanghai city, P.R. China) was added to the gelatin solution at a ratio of 150 g: 1 L (w/v) after the solution had been cooled to  $55^\circ\text{C}$ . The mixture was then transferred to a  $60^\circ\text{C}$  water bath to facilitate dissolution of the antibiotic powder and create a homogeneous clindamycin-gelatin solution. The resultant solution was used to encapsulate the RBX pellet in a stainless mold, each with 0.2 mL of the solution (about 30 mg clindamycin). The encapsulated pellets were coated by immersion for 10 s into a solution of 50 g/L polycaprolactone (PCL)/tetrahydrofuran, which further reduced the rate of antibiotic release. Then the pellets were air-dried. The PCL coating procedure was repeated two more times: the resultant clindamycin-reconstituted bone xenograft-composite (C-RBX-C) pellet, enveloped in a total of three layers of PCL coating, was vented for 48 h, sterilized with ethylene oxide and stored until use. The final weight of each C-RBX-C pellet was about 70 mg.

### Ultrastructure of the Composites

The ultrastructures of cancellous bone granules, RBX, RBX with gelatin, and C-RBX-C were assessed by scanning electron microscopy. The porosity was measured in a gravity bottle (1863 Hubbaru, Shanghai City, and P.R. China) at  $30^\circ\text{C}$  according to Shi et al.<sup>29</sup> In brief: the gravity bottle was filled with ethanol and weighed ( $W_1$ ); the dry composite was weighed ( $W_s$ ) and soaked in the same bottle in ethanol, until every hole of composite was filled with ethanol. Then the bottle was filled up, again, with ethanol and

weighed ( $W_2$ ); the composite was taken out of the bottle, the bottle was weighed again ( $W_3$ ). The porosity of composite was calculated as follows ( $\rho$  being the density of ethanol at that temperature [ $30^\circ\text{C}$ ]):

$$\text{The volume of the scaffold: } V_s = (W_1 - W_2 + W_s)/\rho$$

$$\text{The volume of holes: } V_p = (W_2 - W_3 - W_s)/\rho$$

$$\begin{aligned} \text{The porosity of the scaffold: } \varepsilon &= V_p/(V_p + V_s) \\ &= (W_2 - W_3 - W_s)/(W_1 - W_3) \end{aligned}$$

### Bioassay of C-RBX-C

Thirty-six BALB/c mice (License number SCXK 2002-005, lab animal center of the Fourth Military Medical University) weighing 20–22 g, male, and 6 weeks old, were randomly divided into three groups. C-RBX-C (weighing 70 mg), RBX (weighing 30 mg), and calf cancellous bone (weighing 28.5 mg) were implanted into muscle pouches in the right thighs of 12 mice from each of the groups following a protocol approved by our institutional animal care committee. Six animals of each group were sacrificed at the second and fourth week postoperatively. The samples were harvested and each sample was cut in two halves. One half of the sample mass ( $\sim 300$  mg) was fixed with 100 mL/L formaldehyde, decalcified in 0.1M hydrochloric acid for a period of 1 week, and processed with graded concentrations of alcohol before it was embedded in paraffin and sectioned longitudinally (10  $\mu\text{m}$  thickness). Subsequently, it was stained with hematoxylin and eosin. The other half was homogenized by tissue grinders (Tenbroeck Tissue Grinders, USA) in 0.5 mL phosphate buffer at pH 7.4 and centrifuged at 10,000g for 10 min. Alkaline phosphate (ALP) activity in the supernatant was measured spectrophotometrically (SP-2100UV, Shanghai City, and P.R. China), using the A059 alkaline phosphate detection kit (Nanjing Jiancheng Bioengineering Institute, Nanjing City, and P.R. China) and following the instructions of the manufacturer. Finally the optical results were converted into international units according to the formula that came with a calibration standard provided by the manufacturer.

### Release of Clindamycin From C-RBX-C *In Vivo*

To measure antibiotic release kinetics, C-RBX-C was implanted into the right thigh muscle pouch of 36 BALB/c mice (weighing 20–22 g, male and 6 weeks old), as above. Six animals in each group were sacrificed on postoperative days 0.5, 1, 3, 7, 14, and 21. Just prior to sacrificing the animals,  $\sim 1$  ml of blood was collected by capillary from the venous plexus of the eye ball of each mouse for the detection of blood clindamycin levels. The soft tissue (about 25 mg) surrounding the C-RBX-C implants was excised and homogenized in 0.5 mL of phosphate buffer at pH 7.4 for detecting the local clindamycin level. The levels of clindamycin in both the blood and the tissue were measured by the disc-

diffusion assay,<sup>30</sup> using *Staphylococcus aureus* ATCC28923 as the test bacterium. In this strain of *Staphylococcus*, the minimum inhibitory concentration (MIC) of clindamycin is 0.25  $\mu\text{g/mL}$ .

### Osseous Defect Repaired by C-RBX-C in Rabbit Models

Fifty male New Zealand white rabbits weighing 2.2–2.6 kg (male and 6 months old) were randomly divided into five groups. Under general anesthesia (i.v. injection of 15 mg/kg pentobarbital) an osteoperiosteal defect of 15 mm was created through the whole thickness of the shaft of the right radius by removing the segmental bone. The 0.2 mL of a *Staphylococcus aureus* (ATCC28923) suspension at a concentration of  $5 \times 10^6$  colony forming units (CFU)/mL were injected into each defect. After 30 min the defects were washed with sterile saline. In group A, the defects were filled with three C-RBX-C granules containing 90 mg (each about 30 mg) of clindamycin. And in group B and C, the defects were filled with three RBX granules (weighing as above). Postoperatively, animals of group B received intramuscular clindamycin injection twice per day (at a dosage of 50 mg/Kg) for 5 days. In group D, the defects were filled with three calf cancellous bone granules (weighing as above) and the defects of group E were left empty without any filling material. The ambient muscles held the graft in place, without the need for internal fixation or external splints. Blood samples were taken from the ear vein of the rabbits in group A and B at days 0.5, 1, 3, 7, 14, and 21 for the determination of clindamycin serum levels. At 4, 8, and 16 weeks, 3, 3, and 4 animals of each of the groups were killed for radiological and histological evaluation.

### Microbiological Determination of Clindamycin

Clindamycin concentrations in rabbit serum were measured as described above, using the disc-diffusion assay,<sup>30</sup> with *Staphylococcus aureus* (ATCC28923) as the test bacterium.

### Statistical Analysis

Where appropriate, statistical analyses were performed by one way ANOVA, and the data was presented as the mean  $\pm$  SD. Statistical significance was set at  $p < 0.05$ .

## RESULTS

### Microstructure of the Composites

Scanning electron micrographs of the scaffolds are shown in Figure 1. The basic scaffold [RBX, Figure 1(A)] showed a regular porous structure, containing both big pores (300–500  $\mu\text{m}$  in diameter) and smaller interconnected pores [50–80  $\mu\text{m}$  in diameter, Figure 1(B)], thus closely resembling the structure of cancellous bone. The thickness of the wall

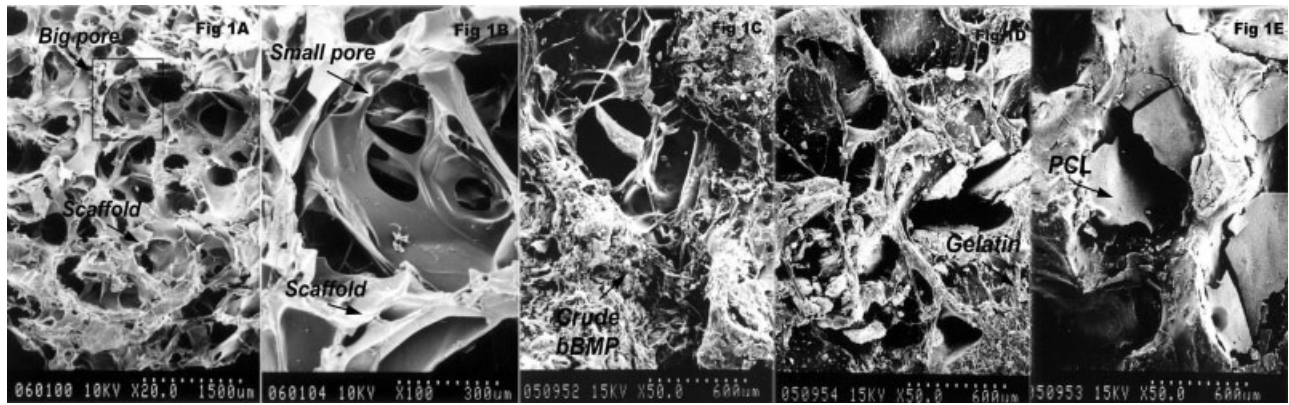


**Figure 1.** Scanning electron micrographs of the various scaffolds. The basic scaffold [RBX, (A)] showed a regular porous structure, containing both big pores (300–500  $\mu\text{m}$  in diameter) and smaller interconnected pores (50–80  $\mu\text{m}$  in diameter) (B). The thickness of the wall between the big pores in the RBX scaffolds was 60–100  $\mu\text{m}$ . A cotton-like appearance of the crude bBMP fraction was found in the pores of the cancellous bone (C). In the composite scaffolds containing gelatin and PCL, the porous structure was partially concealed and covered by gelatin and PCL, respectively (D,E).

between the big pores in the RBX scaffolds was 60–100  $\mu\text{m}$ . A cotton-like appearance of the crude bBMP fraction was seen precipitated in the pores of the cancellous bone [Figure 1(C)]. Figure 1(D,E) show the ultrastructure of composite scaffolds containing gelatin and PCL. We found that the porous structure was covered by gelatin and PCL, which was good for the slow-release of antibiotic and bBMP. Table I summarizes the measured data for porosity and pore size of all our composite scaffolds. We noted that our RBX scaffolds closely resemble native cancellous bone in terms of pore size and porosity.

#### Histological Studies of Crude bBMP

Crude extracts of bBMP were prepared and tested *in vivo*, as described in detail in Materials and Methods. Two weeks after implantation, photomicrograph showed the induction of ectopic bone by crude bBMP in mice and cartilage islands were seen in thigh muscle pouches (Figure 2).

#### Release of Clindamycin From C-RBX-C Scaffolds *In Vivo*

Upon implantation of the antibiotic-soaked scaffolds into the thigh pouch of BALB/c mice, the local levels of clindamycin

**TABLE I.** Pore Size and Porosity of Cancellous Bone and of Composite Scaffolds<sup>a</sup>

	Pore Size ( $\mu\text{m}$ )	Porosity (%)
Common cancellous bone	200–400 <sup>b</sup>	70–80
Cancellous bone granules	Big pores 300–500	87
	Small pores 50–80	
RBX	Big pores 300–500	87
	Small pores 50–80	
With gelatin	300–500	70
C-RBX-C	300–500	48

<sup>a</sup> Pore sizes and porosities were measured as detailed in Materials and Methods.

<sup>b</sup> References 31 and 32.

in the muscle tissue around the C-RBX-C implants were assessed, as detailed in Materials and Methods. As seen in Figure 3(A), local clindamycin concentration was as high as  $997 \pm 123 \mu\text{g/mL}$  12 h after implantation and remained 47 times above the MIC of *Staphylococcus aureus* ( $<0.25 \mu\text{g/mL}$ ) on the 21st day ( $11.8 \pm 3.0 \mu\text{g/mL}$ ). By contrast, and as the systemic controls, serum levels of clindamycin never exceeded a 3.0  $\mu\text{g/mL}$  during the 21 days of the experiment [Figure 3(B)].

In rabbits, the serum concentration of clindamycin in group A reached its peak level ( $2.0 \pm 0.2 \mu\text{g/mL}$ ) 12 h

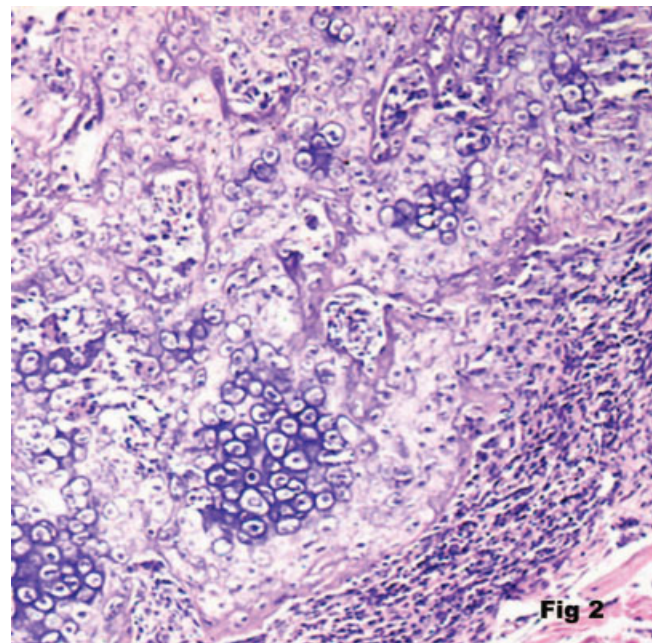


**Figure 2.** Induction of ectopic bone by crude bBMP in mice and cartilage islands in thigh muscle pouches (hematoxylin and eosin staining, original magnification  $\times 400$ ). [Color figure can be viewed in the online issue, which is available at [www.interscience.wiley.com](http://www.interscience.wiley.com).]

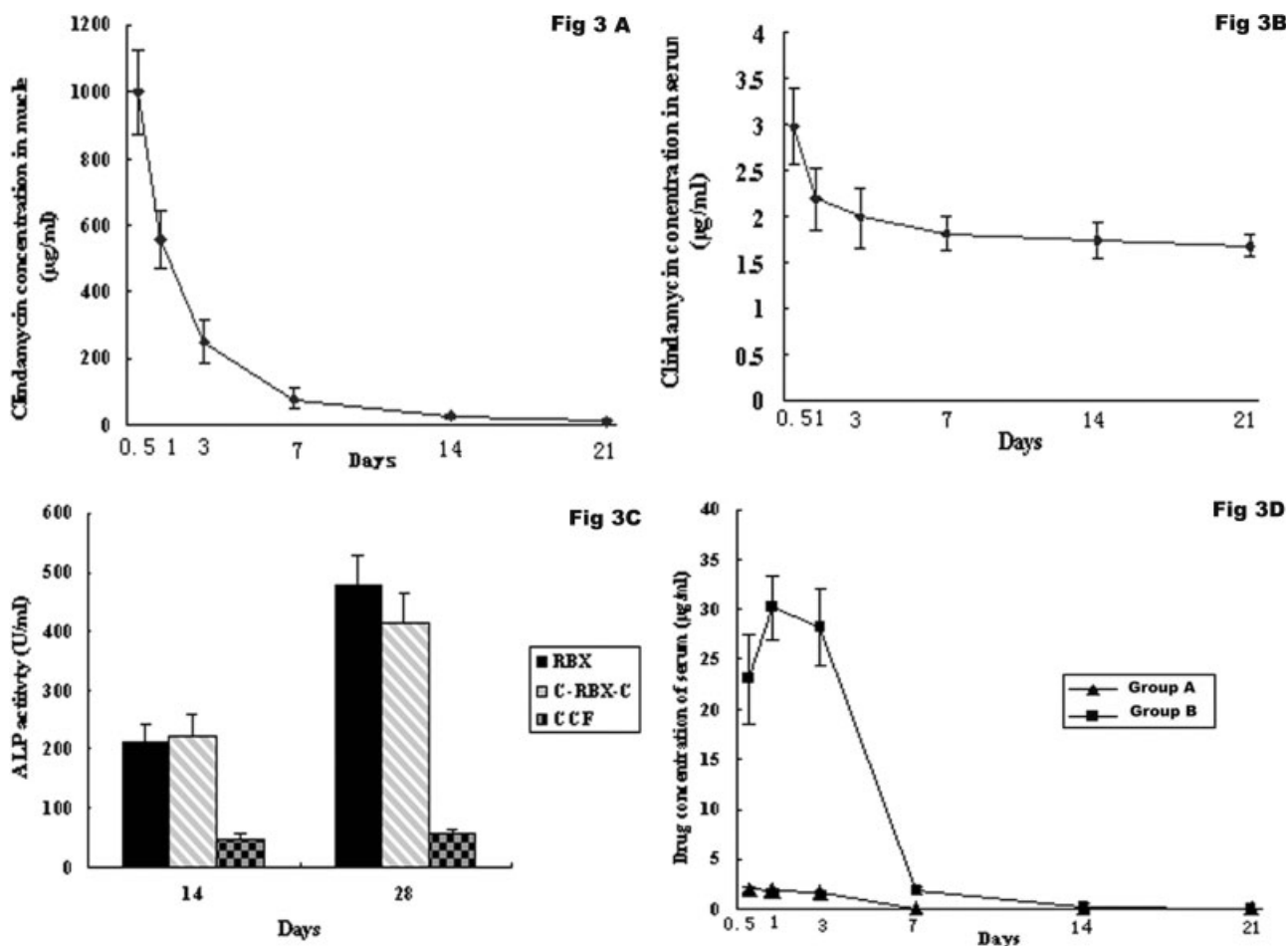


**Figure 3.** Concentration of clindamycin in mice muscles (A) and in serum (B) at various times after implantation of C-RBX-C scaffolds. Shown in (C) is the activity of alkaline phosphatase (ALP) in muscle of animals receiving C-RBX-C, RBX, and calf cancellous framework (CCF) scaffolds, respectively ( $n = 6$ ,  $p < 0.01$  compared with the CCF group). (D) shows the concentration of clindamycin in rabbit serum at various times after implantation of C-RBX-C. All data is shown as mean  $\pm$  SD.

after implantation of C-RBX-C and then slowly decreased. At all times during these studies, serum clindamycin levels were considerably below the toxic range ( $>10 \mu\text{g/mL}$ ). In group B, in which the antibiotics were administered systematically, the serum clindamycin level was initially higher than the toxic range ( $>20 \mu\text{g/mL}$ ) and dropped rapidly after the drug use was discontinued on the 15th day, and could not be examined on the 14th day [Figure 3(D)].

#### Histological Examination of Implants in Mice

Four weeks after implantation of C-RBX-C and RBX into the thigh muscle pouch of mice, islands of cartilage were seen with ossification occurring in the center, and discernible foci of chondroid, osteoid, woven bone, and bone marrow [Figure 4(A)]. By contrast, upon implantation of pure calf cancellous bone only incompletely degraded scaffold material was found in the muscle pouch [Figure 4(B)]. Activity of ALP in the C-RBX-C and RBX implanted animals were significantly higher than that of calf cancellous implantation ( $p < 0.05$ ) [Figure 3(C)].

#### Macroscopic Examination and Bacteriology Studies

All wounds in the rabbits of group A healed completely in 2 weeks [Figure 5(A)]. The wounds of five of the animals in group B and of two animals in group E healed within 3–5 weeks, while the wounds in the other groups failed to heal for more than 5 weeks. The wounds of rabbits in group C, D, and E appeared red and swollen for more than 7 days and there was pus exuding from the wounds [Figure 5(B)]. Upon bacteriological examination, *Staphylococcus aureus* ATCC28923 was detected in the secreted pus. Pus secretion was spontaneous absorption for more than 3 weeks. Of the 50 rabbits used in these studies, five animals died respectively, on the 8th day (one animal in group D), on the 10th day (one animal each of groups C and D), on the 13th day (one animal of group D), and on the 21st day (one animal in group E). Blood from the dead rabbits, sterilely collected from the heart was cultured for 24 h and *Staphylococcus aureus* was detected. Twelve weeks after operation *Staphylococcus aureus* still could be detected in the tissue of bone defect of part rabbits group B (4/10), C (8/10), D (10/10), and E (6/10) by tissue culture, but not in any animals of group A.

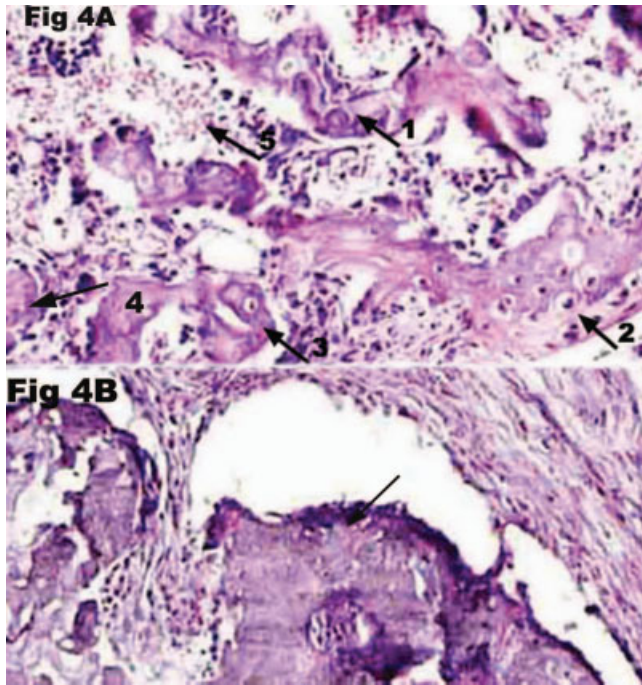


**Figure 4.** Four weeks after implantation of C-RBX-C, islands of cartilage were seen with ossification occurring in the center (arrow 1). Foci of chondroid (arrow 2), osteoid (arrow 3), woven bone (arrow 4), and bone marrow (arrow 5) were observed in the thigh muscle pouch of mice (A). In the control group (pure calf cancellous bone) no ossification was found, while the cancellous bone was incompletely resorbed and degraded, and remnants were surrounded by fibrous tissue (B). (Hematoxylin and eosin staining, original magnification  $\times 100$ ). [Color figure can be viewed in the online issue, which is available at [www.interscience.wiley.com](http://www.interscience.wiley.com).]

### Radiological Findings in Rabbits

As demonstrated in animals of group A, bone callus formed by the 4th week, defects started repairing by the 8th week, and the medullary cavity was recanalized by the 16th week. By comparison, the defects appeared to be nonunion or delayed union in group B (union vs. delayed union vs. nonunion is 2:4:4) and group E (delayed union vs. nonunion is 7:3), and osteomyelitis was seen in group C (10/10) and group D (10/10) even at week 16 (Figure 6).

### Histological Findings in Rabbits

In group A, chondrogenesis and osteogenesis were seen, while no indications of inflammatory infiltration were found 4 weeks postoperatively. On the eighth week, copious new bone tissue was found within and around the graft material. There was obvious creeping substitution in some areas with the graft disorganized, largely resorbed and combined with the new bone. The woven bone, lamellar bone, and recanalization of the marrow cavity were identified in most of the specimens, and the defects were found to have been completely repaired by the 16th week [Figure 7(A)]. In group B, some animals (8/10) receiving bony defects were filled with scar tissue [Figure 7(B)], while the other animals (2/10) were repaired. In Groups C and D, (7/10) and (10/10) animals showed signs of infiltration of chronic inflammatory cells [Figure 7(C,D)], while the remaining material degraded into small fragments and was embedded in the connective tissue [Figure 7(C)]. In group E, the animals (10/10) receiving bony defects were filled with scar tissue.

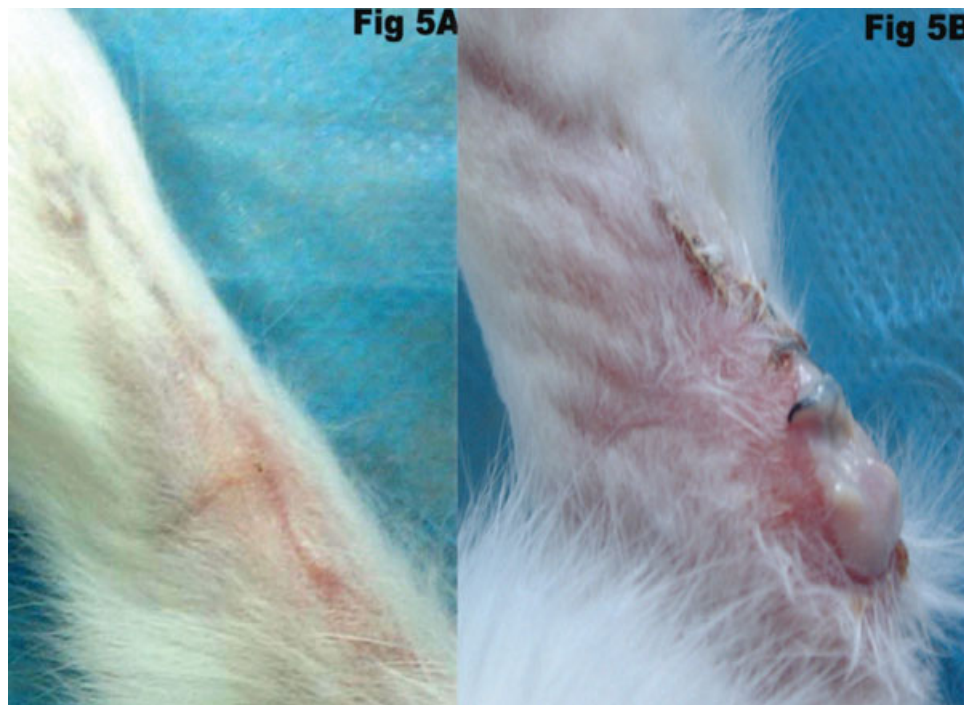


**Figure 5.** The wound of group A healed completely (A), while pus continued to exude from the wounds of rabbits in group C for more than 3 weeks (B). [Color figure can be viewed in the online issue, which is available at [www.interscience.wiley.com](http://www.interscience.wiley.com).]



**Figure 6.** Bone defect repaired medullary cavity recanalized at the 16th week in group A. In comparison, the defects appeared to be nonunion or delayed union in group B, osteomyelitis formed in group C and D, and no bone formed in the defect of group E.

## DISCUSSION

The best treatment of contaminated or infected bone defects is to control infection and repair bone defect at the same time. This dual task requires an osteoinductive bone graft composite with antibiotic release capabilities, good porosity, and osteogenesis-matched degradation properties.<sup>33</sup>

The formation of new bone and degradation of the planted material are all affected by the porous structure and organization of optimized scaffold material, which should promote the ingrowth of bone tissue into the matrix and also encourage vascularization and bone remodeling.<sup>34,35</sup> RBX possesses a porous structure with large pores ranging between 300 and 500  $\mu\text{m}$  in diameter, and a porosity of 87%. This combination of pore size and porosity appears to be most desirable for a biomaterial-based carrier to be used in bone repair.<sup>31,32</sup> To mimic the osteoinductive property of natural bone as graft material, crude bone morphogenetic protein (BMP) was incorporated into RBX. BMP, first described by Urist<sup>36</sup> is an effective local stimulator of bone healing.<sup>37,38</sup> Previous studies suggested that the composition and architecture of the carrier affect bone healing processes,<sup>39</sup> although the osteoinductive properties of BMP may be independent of the type of carrier material. As seen in Figure 1(A), RBX has an innate macroporous structure with regular interconnected microspores and regular pore sizes, which facilitate ingrowth of the neotissues. The matrix contained in the RBX scaffolds provides bBMP with an optimal combination of a suitable matrix, which not only facilitates cell adhesion to the scaffold but also acts as slow-release depot, thus enhancing the role of crude bBMP as an osteoinductive agent, as also confirmed in previous studies.<sup>23,40</sup> The findings in this study indicate that the porous nature of the RBX scaffold effectively supports the biological function of crude bBMP. We also found that the

degradation of pure cancellous granule without crude bBMP (in group D) was slower than RBX (with crude bBMP in group A, B, and C) (Figure 7), suggesting that the presence of crude bBMP may accelerate the resorption of the carrier and the induction of new bones formation. Our results indicate an inverse relationship between the percentage of residual material (cancellous bone) and new bone formation in the preexisting defect.

Xenograft and allograft are related to biohazard infection risk. And many studies on synthetic biomaterials with antimicrobial properties (e.g. bioactive glass) have been done both experimentally and clinically.<sup>41,42</sup> The synthetic biomaterials used for clinical purposes demands many special properties, such as osteoinductive and osteoconductive abilities. We have also done some studies on synthetic biomaterials,<sup>43–46</sup> and found that there was not a synthetic biomaterial that could provide all the above characteristics. Bioceramics cannot be degraded completely and become a block of bone formation. Polymers have poor strength and can create aseptic exudation by releasing acid matter. However, we do believe that with the development of biomaterial technology, synthetic biomaterials can completely imitate and substitute for nature bone grafts in the future.

Effective anti-infection action is another important function of the C-RBX-C matrix. *Staphylococcus aureus* is reportedly the main pathogen in bone infection.<sup>34,35</sup> Clindamycin has excellent *in vitro* activity against most strains of

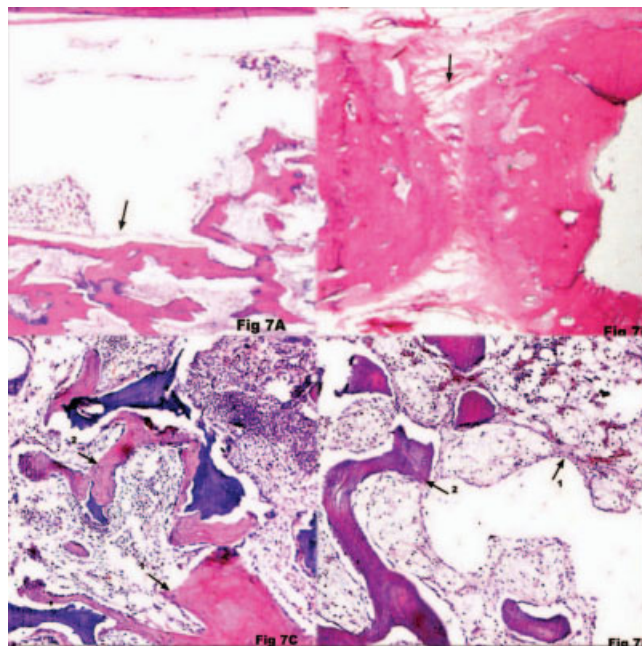


**Figure 7.** At the 16th week, ossification and medullary cavity recanalized in group A (A), nonunion and the bony defects were filled with scar tissue in group B and E (B). In group C, the remaining material degraded into small fragments (arrow 1) and was embedded in the connective tissue, new bone ossification was also found in the center (arrow 2) (C). In group D, infiltration of chronic inflammatory cells (arrow 1) and plenty of incompletely resorbed and degraded remnants (arrow 2) were noted (D). [Color figure can be viewed in the online issue, which is available at [www.interscience.wiley.com](http://www.interscience.wiley.com).]

*Staphylococcus aureus* and is not inactivated by  $\beta$ -lactamase. With excellent penetrability in osseous tissue, clindamycin can penetrate into micro abscesses of infected tissues and inhibit bacterial growth.<sup>47</sup> It can be used orally as well as by intramuscular and intravenous injections where the recommended dose is 600–900 mg/8 h.<sup>48,49</sup> Just like other antibiotics, clindamycin can cause numerous allergic reactions, such as a skin ulcer, diarrhea, and even shock. The most common adverse effects of clindamycin are pseudomembranous colitis and diarrhea<sup>50,51</sup>; however, when used locally, such as in local drug (antibiotic) delivery systems (LDDS), these adverse effects may be prevented. Unlike penicillin's, in China, skin testing is not required for the use of clindamycin, which is another reason for using this antibiotic in our study.

Bacterial antibiotic resistance is a troublesome problem in the clinical practice. There are many reasons for the emergence of this resistance, the long time use of low doses of antibiotics being an important one. If the bacteria cannot be killed with an effective concentration of a given antibiotic in a short time, antibiotic resistance will occur due to the mutation of the bacteria.<sup>52</sup> In our study, high local doses of clindamycin were achieved rapidly upon implanting the composite scaffolds due to the slow release properties of the scaffold, antibiotic levels remained significantly above the MIC (minimal inhibitory concentration) for *Staphylococcus aureus* so that the bacteria could be killed immediately concomitantly with shutting off the pathways leading to antibiotic resistance. In our study, we used *Staphylococcus aureus* ATCC28923 as the test bacterium, which has a MIC value for clindamycin of 0.25  $\mu\text{g}/\text{mL}$ . Our data clearly indicates that at any given time the available local concentration of clindamycin at the site of the infection exceeded 0.25  $\mu\text{g}/\text{mL}$ . Furthermore, clindamycin can modulate inflammatory-cytokine induction in lipopolysaccharide-stimulated mice, which maybe useful for controlling osteonecrosis by excessive inflammatory reaction of infected tissue.<sup>53</sup>

One of the major challenges of this study was to ensure that clindamycin has no adverse effect on the osteoinductive power of crude bBMP, given its sensitivity to thermal processing, sterilization procedures, and the action of some chemicals.<sup>54</sup> Using our bioassay, we found in preliminary tests, that 180 g/L of clindamycin in gelatin solution can inhibit the osteoinductive capability of crude bBMP. Ectopic bone formation could not be observed at clindamycin concentrations of >200 g/L. In the current study, when clindamycin (150 g/L) was dissolved in a gelatin solution we did not observe any inhibition of ectopic bone formation, suggesting that C-RBX-C with an optimal concentration of clindamycin might be effectively used for protecting bone grafts against bacterial infections. To prevent a buildup of drug resistance through long-term use of clindamycin, we also evaluated, as a control for multiple bacterial bone infections, the effects of other antibiotics such as gentamicin,<sup>55</sup> ciprofloxacin, and rifampicin on crude bBMP function. Having determined

optimal concentrations (safe to patient and effective for the bacteria) for each of the above antibiotics, we did not observe any adverse effects (such as toxics, diarrhea, allergic reactions, and so on). Clindamycin is widely used for the treatment of infections caused by gram-positive bacteria such as *Staphylococcus aureus*. In clinical practice, both gram-negative and gram-positive infections are frequently encountered. In this study, we report on the efficacy of clindamycin in our composite. Taken together, our results show that with our technology we can create composite bone graft materials with anti-infective proclivity; these composite grafts contain suitable antibiotics which are effective against a variety of musculoskeletal infections.

Sustained release of antibiotics plays an important role for curative effect of LDDS.<sup>56</sup> In order to enhance the slow-release characteristics of C-RBX-C; the composite was encapsulated in gelatin and polycaprolactone. Using a mouse model, we were able to detect, 21 days postoperatively, a local concentration of 11.8  $\mu\text{g}/\text{mL}$  of clindamycin which was 47 times higher than the MIC of *Staphylococcus aureus*. Importantly, the serum concentration of clindamycin remained below the toxic range ( $\sim 10$   $\mu\text{g}/\text{mL}$ ) [Figure 3(B)]. In our study, safety and efficacy of scaffold associated clindamycin was better than previously reported.<sup>55</sup> When comparing serum levels of clindamycin between groups A and B [Figure 3(D)], we found that antibiotics administration in the form of LDDS was safer and more effective in treating bone infection than systemic administered. These results confirm recent findings by Gil-Albarova et al.<sup>57</sup>

The cortical bone defect model in a rabbit has been used in this study to observe the repair ability of C-RBX-C in treating a 15 mm segmental bone defect, which cannot heal spontaneously.<sup>58,59</sup> In our experimental groups D and E (untreated controls), we failed to see any bone repair and found only fibro-vascular connective tissue filling the defects.

To imitate infectious bone defect, we infected the bone defects with  $5 \times 10^6$  CFU/mL *Staphylococcus aureus*, and left the bacterial inoculums *in situ* for another 30 min. This procedure has previously been shown to yield significant levels of bacterial infections.<sup>33,59</sup> The pus exuding from the wounds after 3 days and bacterial cultures taken from animals in groups C and D, indicated that we had indeed successfully created a valid infective bone defect model.

Numerous previous studies have employed BMP and cancellous bone grafts, either alone or in combination, in order to enhance bone healing. In our study, we believe that each and every component of our composite is important. BMP is an effective cytokine for osteoinduction, while the natural scaffold of cancellous bone is important for osteoconduction and degradation, which occurs during formation of new bone. Finally, antibiotics, such as clindamycin, can effectively control bone infection. Most importantly, we have created an effective technology for packaging compound cytokines, scaffolds, and antibiotics. By changing one of the components, we can now generate different composites which can be customized according to

individual needs and requirements of patients suffering from distinct infectious bone defects.

To summarize, C-RBX-C as a LDDS for treating contaminated or infective bone defects and osteomyelitis, displays several advantages. First, slow, sustained release of the antibiotic at the site of infection yields elevated local concentrations, while minimizing any risk of systemic toxicity. Second, a variety of antibiotics can be selected to cover both gram negative and positive bacteria, thereby facilitating individualized chemotherapy. Third, the biodegradability of the scaffold materials eliminates the need for a second surgical procedure for their removal. Finally, and most important, enhanced osteoinductivity of the scaffolds can resolve the dilemma of bone grafts. In order to translate this technology into the clinic, further, more detailed, studies are needed.

Many thanks to Dr. Lelkes, the Calhoun Chair Professor of Cellular Tissue Engineering, School of Biomedical Engineering, Science and Health Systems of Drexel University, Philadelphia, PA for his help with the correction of the grammar and spelling errors of the original manuscript.

## REFERENCES

- Korkusuz F, Korkusuz P, Eksioglu F, Gursel I, Hasirci V. In vivo response to biodegradable controlled antibiotic release systems. *J Biomed Mater Res* 2001;55:217–228.
- Shinto Y, Uchida A, Korkusuz F, Araki N, Ono K. Calcium hydroxyapatite ceramic used as a delivery system for antibiotics. *J Bone Joint Surg Br* 1992;74:600–604.
- Cornell CN, Tyndall D, Waller S, Lane JM, Brause BD. Treatment of experimental osteomyelitis with antibiotic-impregnated bone graft substitute. *J Orthop Res* 1993;11:619–626.
- Gerhart TN, Roux RD, Horowitz G, Miller RL, Hanff P, Hayes WC. Antibiotic release from an experimental biodegradable bone cement. *J Orthop Res* 1988;6:585–592.
- Garvin K, Feschuk C. Polylactide-polyglycolide antibiotic implants. *Clin Orthop Relat Res* 2005;437:105–110.
- Kanellakopoulou K, Giamarellos-Bourboulis EJ. Carrier systems for the local delivery of antibiotics in bone infections. *Drugs* 2000;59:1223–1232.
- Holtom PD, Patzakis MJ. Newer methods of antimicrobial delivery for bone and joint infections. *Instr Course Lect* 2003;52:745–749.
- Wahlig H. Gentamicin-PMMA-beads: A drug delivery system in the treatment of chronic bone and soft tissue infections. *J Antimicrob Chemother* 1982;10:463–465.
- Stabile DE, Jacobs AM. Development and application of antibiotic-loaded bone cement beads. *J Am Podiatr Med Assoc* 1990;80:354–359.
- Perry A, Mahar A, Massie J, Arrieta N, Garfin S, Kim C. Biomechanical evaluation of kyphoplasty with calcium sulfate cement in a cadaveric osteoporotic vertebral compression fracture model. *Spine J* 2005;5:489–493.
- Stevens CM, Tetsworth KD, Calhoun JH, Mader JT. An articulated antibiotic spacer used for infected total knee arthroplasty: A comparative in vitro elution study of Simplex and Palacos bone cements. *J Orthop Res* 2005;23:27–33.
- Yamanura K, Iwata H, Yotsuyanagi T. Synthesis of antibiotic-loaded hydroxyapatite beads and in vitro drug release testing. *J Biomed Mater Res* 1992;26:1053–1064.
- El-Ghannam A. Bone reconstruction: From bioceramics to tissue engineering. *Expert Rev Med Devices* 2005;2:87–101.
- Jacob E, Cierny G, Zorn K, McNeill JF, Fallon MT. Delayed local treatment of rabbit tibial fractures with biodegradable cefazolin microspheres. *Clin Orthop Relat Res* 1997;336:278–285.
- Garvin KL, Miyano JA, Robinson D, Giger D, Novak J, Radio S. Polylactide/polyglycolide antibiotic implants in the treatment of osteomyelitis: A canine model. *J Bone Joint Surg Am* 1994;76:1500–1506.
- Kim HW, Knowles JC, Kim HE. Hydroxyapatite/poly ( $\epsilon$ -caprolactone) composite coatings on hydroxyapatite porous bone scaffold for drug delivery. *Biomaterials* 2004;25(7/8):1279–1287.
- Gazdag AR, Lane JM, Glaser D, Forster RA. Alternatives to autogenous bone graft: Efficacy and indications. *J Am Acad Orthop Surg* 1995;3:1–8.
- Giannoudis PV, Dinopoulos H, Tsiridis E. Bone substitutes: An update. *Injury* 2005;36(Suppl 3):S20–S27.
- Liu Wei, Hu Yunyu, Lu Yupu, Wang Yuqing. Development and biological activity analysis of reconstituted bone xenograft. *Natl Med J China* 1991;71:378–380.
- Li Dan Sang Hongxun, Hu Yunyu, Yan Zhi, Yang Liu, Ma Shengbin. The effect of technological improvements on yield rate and bioactivity of the product in bBMP extraction. *Orthop J China* 2001;8:576–578.
- Li Yafei, Hu Yunyu, Li Xuebing, Yang Guang, Cong Rui, Li Huanlin. Influence of geometry of bone particles and intensely stirring of the extraction on the yield of bBMP and its osteoinductivity. *Chin J Orthop* 1996;16:118–120.
- Guo Zheng, Hu Yunyu, Lin Yinghua. Ultrastructural observation of heterotopic bone formation induced by bovine bone morphogenetic protein. *J Fourth Milit Med Univ* 1996;17:407–411.
- Hu YY. Experimental studies on reconstituted bone xenograft and its clinical application. *Zhonghua Wai Ke Za Zhi* 1993;31:709–713.
- Urist MR. Bone: Formation by autoinduction. 1965. *Clin Orthop Relat Res* 2002;395:4–10.
- Urist MR, Mikulski A, Lietze A. Solubilized and insolubilized bone morphogenetic protein. *Proc Natl Acad Sci USA* 1979;76:1828–1832.
- Urist MR, Chang JJ, Lietze A. Preparation and bioassay of bone morphogenetic protein and polypeptide fragments. *Methods Enzymol* 1987;146:294–312.
- Ohta H, Wakitani S, Tensho K, Horiuchi H, Wakabayashi S, Saito N, Nakamura Y, Nozaki K, Imai Y, Takaoka K. The effects of heat on the biological activity of recombinant human bone morphogenetic protein-2. *J Bone Miner Metab* 2005;23:420–425.
- Miki T, Imai Y. Osteoinductive potential of freeze-dried, biodegradable, poly (glycolic acid-co-lactic acid) disks incorporated with bone morphogenetic protein in skull defects of rats. *Int J Oral Maxillofac Surg* 1996;25:402–406.
- Shi Guixin, Wang Shenguo, Bei Jianzhong. Preparation of porous cell scaffolds of poly (L-lactic acid) and poly (L-lactic-co-glycolic acid) and the measurement of their porosity. *J Funct Polym* 2001;149:7–11.
- Chaitram JM, Jevitt LA, Lary S, Tenover FC. The World Health Organization's External Quality Assurance System Proficiency Testing Program has improved the accuracy of antimicrobial susceptibility testing and reporting among participating laboratories using NCCLS methods. *J Clin Microbiol* 2003;41:2372–2377.
- Yoshimoto H, Shin YM, Terai H, Vacanti JP. A biodegradable nanofiber scaffold by electrospinning and its potential for bone tissue engineering. *Biomaterials* 2003;24:2077–2082.

32. Herold RW, Pashley DH, Cuenin MF, Niagro F, Hokett SD, Peacock ME, Mailhot J, Borke J. The effects of varying degrees of allograft decalcification on cultured porcine osteoclast cells. *J Periodontol* 2002;73:213–219.
33. Beardmore AA, Brooks DE, Wenke JC, Thomas DB. Effectiveness of local antibiotic delivery with an osteoinductive and osteoconductive bone-graft substitute. *J Bone Joint Surg Am* 2005;87:107–112.
34. Redondo LM, Garcia Cantera JM, Verrier Hernandez A, Vaquero PC. Effect of particulate porous hydroxyapatite on osteoinduction of demineralized bone autografts in experimental reconstruction of the rat mandible. *Int J Oral Maxillofac Surg* 1995;24:445–448.
35. Dai Honglian, L I Shipu, Yan Yuhua, Li Xiaoxi, Jia Li. The osteogenesis process of tricalcium phosphate ceramics in vivo. *Trans Nonferrous Met Soc China* 2003;13:65–68.
36. Urist MR. Bone: Formation by autoinduction. *Science* 1965;150:893–899.
37. Matthews SJ. Biological activity of bone morphogenetic proteins (BMPs). *Injury* 2005;36 (Suppl 3):S34–S37.
38. De Biase P, Capanna R. Clinical applications of BMPs. *Injury* 2005;36(Suppl 3):S43–S46.
39. Dutta Roy T, Simon JL, Ricci JL, Rekow ED, Thompson VP, Parsons JR. Performance of hydroxyapatite bone repair scaffolds created via three-dimensional fabrication techniques. *J Biomed Mater Res A* 2003;67:1228–1237.
40. Wang ZG, Liu J, Hu YY, Meng GL, Jin GL, Yan Z, Wang HQ, Dai XW. Treatment of tibial defect and bone nonunion with limb shortening with external fixator and reconstituted bone xenograft. *Chin J Traumatol* 2003;6:91–98.
41. Meseguer-Olmo L, Ros-Nicolas M, Vicente-Ortega V, Alcaraz M, Clavel M, Arcos D, Vallet-Regi M, Meseguer-Ortiz C. A bioactive sol-gel glass implant for in vivo gentamicin release. Experimental model in rabbit. *J Orthop Res* 2006;24:454–460.
42. Salvi GE, Mombelli A, Mayfield L, Andrea ML, Rutar AS, Jean GS, Lang NP. Local antimicrobial therapy after initial periodontal treatment. *J Clin Periodontol* 2002;29:540–550.
43. Hu Y, Zhang C, Zhang S, Xiong Z, Xu J. Development of a porous poly(L-lactic acid)/hydroxyapatite/collagen scaffold as a BMP delivery system and its use in healing canine segmental bone defect. *J Biomed Mater Res A* 2003;67:591–598.
44. Sun L, Hu YY, Xiong Z, Wang WM, Pan Y. Repair of the radial defect of rabbit by polyester/tricalcium phosphate scaffolds prepared by rapid prototyping technology. *Zhonghua Wai Ke Za Zhi* 2005;43:535–539.
45. Liu G, Hu YY, Zhao JN, Wu SJ, Xiong Z, Lu Rong. Effect of type I collagen on the adhesion, proliferation, and osteoblastic gene expression of bone marrow-derived mesenchymal stem cells. *Chin J Traumatol* 2004;7:358–362.
46. Hu YY, Zhang C, Lu R. Repair of radius defect with bone-morphogenetic-protein loaded hydroxyapatite/collagen-poly (L-lactic acid) composite. *Chin J Traumatol* 2003;6:67–74.
47. Mader JT, Adams K, Morrison L. Comparative evaluation of Cefazolin and Clindamycin in the treatment of experimental *Staphylococcus aureus* osteomyelitis in rabbits. *Antimicrob Agents Chemother* 1989;33:1760–1764.
48. Flaherty JF, Rodondi LC, Guglielmo BJ, Fleishaker JC, Townsend RJ, Gambertoglio JG. Comparative pharmacokinetics and serum inhibitory activity of clindamycin in different dosing regimens. *Antimicrob Agents Chemother* 1988;32:1825–1829.
49. Foppa CU, Bini T, Gregis G, Lazzarin A, Esposito R, Moroni M. A retrospective study of primary and maintenance therapy of toxoplasmic encephalitis with oral clindamycin and pyrimethamine. *Eur J Clin Microbiol Infect Dis* 1991;10:187–189.
50. Brook I. Pseudomembranous colitis in children. *J Gastroenterol Hepatol* 2005;20:182–186.
51. Xu Xiaogang, Li Guanghui. Guidelines of antimicrobial agent prophylaxis in surgery. *Chin J Infect Chemother* 2005;5:180–183.
52. Schentag JJ, Gilliland KK, Paladino JA. What have we learned from pharmacokinetic and pharmacodynamic theories? *Clin Infect Dis* 2001;32(Suppl 1):S39–S46.
53. Nakano T, Hiramatsu K, Kishi K, Hirata N, Kadota J, Nasu M. Clindamycin modulates inflammatory-cytokine induction in lipopolysaccharide-stimulated mouse peritoneal macrophages. *Antimicrob Agents Chemother* 2003;47:363–367.
54. Heckman JD, Ehler W, Brooks BP, Aufdemorte TB, Lohmann CH, Morgan T, Boyan BD. Bone morphogenetic protein but not transforming growth factor- $\beta$  enhances bone formation in canine diaphyseal nonunions implanted with a biodegradable composite polymer. *J Bone Joint Surg Am* 1999;81:1717–1729.
55. Li XD, Hu YY. The treatment of osteomyelitis with gentamicin-reconstituted bone xenograft-composite. *J Bone Joint Surg Br* 2001;83:1063–1068.
56. Zalavras CG, Patzakis MJ, Holtom P. Local antibiotic therapy in the treatment of open fractures and osteomyelitis. *Clin Orthop Relat Res* 2004;427:86–93.
57. Gil-Albarova J, Salinas AJ, Bueno-Lozano AL, Roman J, Aldini-Nicolo N, Garcia-Barea A, Giavaresi G, Fini M, Giardino R. The in vivo behaviour of a sol-gel glass and a glass-ceramic during critical diaphyseal bone defects healing. *Biomaterials* 2005;26:4374–4382.
58. Dodde R II, Yavuzer R, Bier UC, Alkadri A, Jackson IT. Spontaneous bone healing in the rabbit. *J Craniofac Surg* 2000;11:346–349.
59. Garvin KL, Hanssen AD. Infection after total arthroplasty. Past, present, and future. *J Bone Joint Surg Am* 1995;77:1576–1588.